Title

Mass-transport resistances of acid and alkaline ionomer layers: A microelectrode study part 1 - Microelectrode development

Journal

ECS Transactions, 92(8)

ISSN

1938-6737

Authors

Petrovick, JG
Kushner, DI
Tesfaye, M
et al.

Publication Date

2019

DOI

10.1149/09208.0077ecst

Peer reviewed

Mass-Transport Resistances of Acid and Alkaline Ionomer Layers: A Microelectrode Study
Part 1 - Microelectrode Development

J. G. Petrovick[a,b], D. I. Kushner[b], M. Tesfaye[a,b], N. Danilovic[b], C. J. Radke[a], and A. Z. Weber[b]

[a] Department of Chemical and Biomolecular Engineering, University of California, Berkeley, CA 94704, USA

[b]Energy Conversion Group, Lawrence Berkeley National Laboratory, Berkeley, CA 94720, USA

The use of microelectrodes to study localized mass-transport phenomena in fuel-cell catalyst layers is an increasingly valuable tool. However, existing microelectrode cells have been used in static, equilibrated environment modes with poorly controlled interfaces. In this work, we present a microelectrode cell design that expands the experimental space addressable by microelectrodes to include mechanical pressure, gas flow and ionomer medium, and experimental throughput. The feasibility of the design is examined for fuel-cell reactions, with oxygen reduction currents independent of mechanical pressure and gas flowrate. Finally, cell equilibration time and IR drop across the electrolyte are estimated. The new cell design is robust and provides a consistent base from which to perform more complicated studies examining mass-transport properties of ionomers and/or the electrochemical reaction kinetics of hydrogen oxidation and oxygen reduction.

Introduction

One of the most important research areas currently in polymer-electrolyte fuel cells (PEFCs) is the study of interactions between catalyst and ionomer within the PEFC catalyst layer. These layers consist of platinum-loaded carbon particles embedded in a thin film of ionomer, typically Nafion®. The study of the oxygen-reduction (ORR) and hydrogen-oxidation reactions (HOR) in these layers, as well as mass transport of gases through the ionomer film encapsulating the Pt catalyst particles, allows for more efficient catalyst layers, and therefore more efficient PEFCs. This is especially true for ultra-low Pt loadings, where the limiting factor appears to be localized mass transport of O_2 through the ionomer film (1). One proposed way of studying these phenomena is to use microelectrodes to mimic the heterogeneous interfaces in the PEFC (2). Microelectrodes are sub-milometer electrodes that allow well-defined electrochemical measurements to be performed in a non-liquid (that is, a humidified solid ionomer) electrolyte environment (2). Additional advantages of this setup include minimization of the IR drop between electrodes, due to the low current, and a diffusion layer larger than the scale of the microelectrode (3).

In the case of catalyst layers, microelectrodes act as a model analogue, allowing for the study of HOR and ORR in a more controlled and defined environment and architecture

than in a typical fuel cell (2, 4). Many studies have used microelectrodes to study Nafion and these electrochemical reactions, covering a wide range of topics, but most have focused on ORR (1, 2, 4, 5). Some researchers studied the mass-transport characteristics of oxygen gas in Nafion or the platinum/ionomer interface (1, 5, 6), whereas others focused on the kinetics of the reaction itself on the electrode (4, 7, 8). Commonly, the microelectrode setups are complex and the ionomer requires a long equilibration time with the desired temperature, pressure, and relative humidity (RH); in some cases, exceeding 12 hours (2, 5). The second challenge is the placement of the counter and reference electrodes without perturbation of the working-electrode measurement, including impeding mass transport, reference shifts, and overpotential losses due to long electrolyte bridges (2, 5).

In this work, we present a new microelectrode-cell design that allows probing and mitigation of these potential measurement issues. Basic experimental procedures are performed, showing its effectiveness for both HOR and ORR. In addition, the effect of applied pressure on electrochemically active surface area (ECSA) and ORR is studied, as well as the effect of gas flowrate, equilibration times, and IR drop. Our design provides a foundation for further work performed in this area.

Experimental

Experimental Setup

The microelectrode cell was designed using Solidworks CAD software and fabricated from co-polyester, using a 3D printer (Ultimaker, Netherlands) for rapid prototyping purposes. The working electrode (WE) was a 50-µm platinum ultramicroelectrode (UME, Bioanalytical Systems, Inc, West Lafayette, IN, USA), the counter electrode (CE) was a platinum mesh (Alfa Aesar, Ward Hill, MA, USA) coated with Nafion (1), while the reference electrode (RE) was a commercial dynamic hydrogen electrode (DHE, Gaskatel, Germany). Nafion 211 (Ion Power, New Castle, DE, USA) was used as the solid-state electrolyte and was pretreated (boiling and acid exchange (9)). Mechanical pressure was monitored using a piezoresistive force sensor (Tekscan, South Boston, MA, USA) interfaced with an Arduino readout. Placement and spacing of the WE, CE, and RE minimize the distance between the WE/CE and RE and allow for gas flow through the CE while also isolating the WE/CE and RE compartments. Measurements in liquid electrolyte were performed with the commercial DHE, Pt microelectrode, and a Pt wire (0.5 M sulfuric acid). The microelectrode was plated with Pt prior to use, using a solution of chloroplatinic acid, hydrochloric acid, and deionized water. The WE was placed in the plating solution, along with a 35.6 x 5.7 mm Pt mesh CE, and 2 V were applied for ~1 min to plate the electrode. All glassware was acid cleaned, and measurements were taken to control UME cleanliness throughout plating, handling, and storage.

Electrochemical Measurements

All electrochemical measurements were performed with an SP-150 potentiostat with a low current card (Bio-Logic, France) at room temperature. Gases were fed by a mass flow controller (MKS, Andover, MA, USA) either dry or through a humidifier (Fuel Cell Technologies, Albuquerque, NM, USA) before entering the microelectrode cell. Gas flow was maintained throughout the entirety of the experiments. For ECSA measurements,

cyclic voltammetry (CV) was performed under humidified argon from 0 to 1.4 V vs DHE at a scan rate of 50 mV/s. ECSA was calculated by integrating under the hydrogen desorption peak (in the range of ~0-0.43 V vs DHE) after subtracting the capacitive background current to find the total surface charge, then normalizing by a standard hydrogen monolayer charge of 210 $\mu C/cm^2$ (5). For HOR and ORR kinetic measurements, cyclic voltammetry was performed using 2% H_2 in Ar and 4% O_2 in nitrogen, respectively, from 0 to 1 V vs DHE at a scan rate of 20 mV/s. All chronoamperometric holds were performed at 0.5 V vs DHE and held for 5 min. The current for these holds was determined by averaging the last 100 s of the hold. Impedance spectroscopy was performed at 0.5 V vs DHE from 100 mHz to 1 MHz. The amplitude was 10 mV.

Results and Discussion

Microelectrode Cell Design

A CAD rendered image of the microelectrode cell is shown in Figure 1. Briefly, our design consists of two separate chambers, one for the working and counter electrodes and one for the reference electrode, with a small path between the two chambers for the reference bridge to pass and make ionic contact (Figure 1a). The counter electrode is placed on the bottom of the larger chamber, and the reference bridge (Nafion 211) is placed on top of it, with its other end placed in the reference electrode chamber. Two Viton O-rings are used to seal the chambers and prevent gas leakage. Gas enters and exits each chamber through gas inlet/outlet ports at the chamber edges; gas tubes can be attached to larger ports on the side of the overall cell (Figure 1c). Each chamber has its own set of channels, allowing for different gases to be fed in each one. When using the commercial DHE the reference flow ports are closed.

A two-piece lid, shown as red in Figure 1a, serves to guide and compress the WE and RE to the base using screws while also sealing the cell against gas leakage. A two-piece cell top compartment is used because the screws and both electrodes pass through O-rings in the lid to provide additional protection against gas leakage. Both the working electrode and DHE pass through this top compartment and press directly into the reference bridge, completing the cell (Figure 1b). Nafion acts both as an electrolyte bridge and as the ionomer interface with the Pt UME. Contact is made with the CE by a wire fed out through the gas outlet port. Pressure is applied to the WE and RE using high precision screws to maintain consistent electrode contact using an external frame structure, not shown. Pressure on the WE is measured *in situ* by placing the piezoresistive force sensor between the microelectrode and high precision screw.

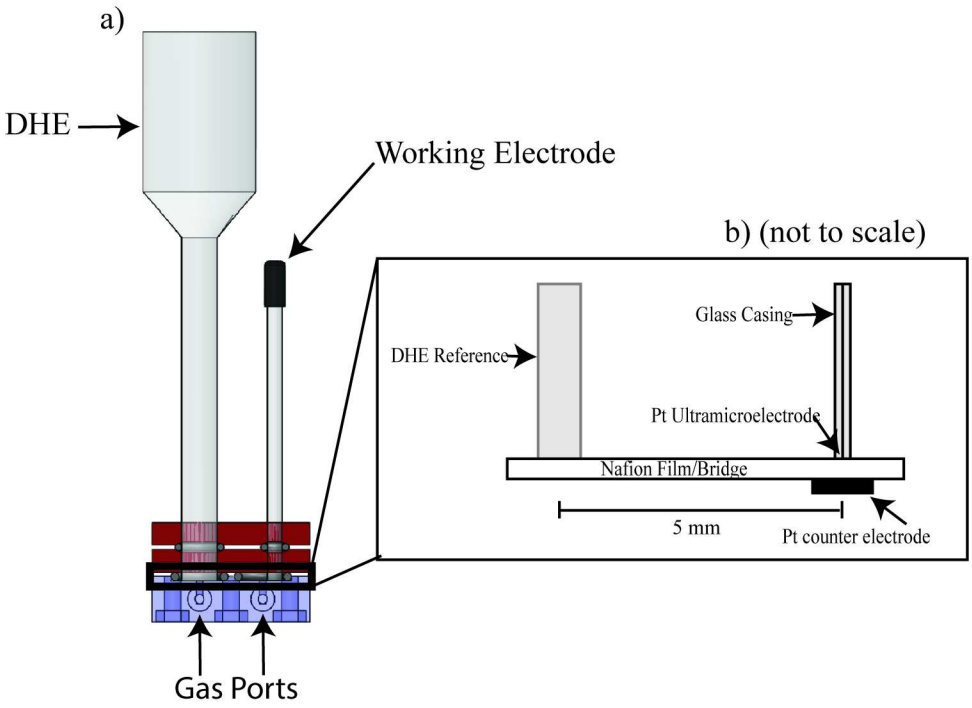

Figure 1. Schematic of microelectrode cell design. a) shows a cross-section from the side. The front and back of the UME cell each have a gas port for each chamber providing an inlet and outlet. b) shows a detailed layout of the components that make the cell circuit.

Design Feasibility

After plating the UME, we performed cyclic voltammetry at a scan rate of 50 mV/s in a liquid electrolyte cell under argon and compared to the same conditions in the microelectrode cell. The gases were humidified at ~95% and 1.38 MPa (200 psi) was applied to the working electrode when the solid-state cell was used. Results are seen in Figure 2. There is good agreement between the CVs in sulfuric acid and the Nafion in the UME cell. In argon, these currents are primarily derived from hydrogen adsorption/desorption and oxide formation/reduction (3). A small (~20 mV) reference shift is also seen when using the solid-state cell compared to aqueous. This is likely a result of a mixed-junction potential in the reference chamber.

When 2% hydrogen gas is used in the UME cell, a positive shift in current in the CV is seen compared to under Ar. This likely comes from the positive contribution of the hydrogen oxidation current. An apparent reduction in OH adsorption occurs during HOR, seen in the smaller area contained in the CV near 1 V vs DHE compared to ORR or under Ar, but the reason for this is unknown. Similarly, when 4% oxygen gas is used, a negative shift in the CV is observed, likely caused by the negative contribution of the oxygen reduction current.

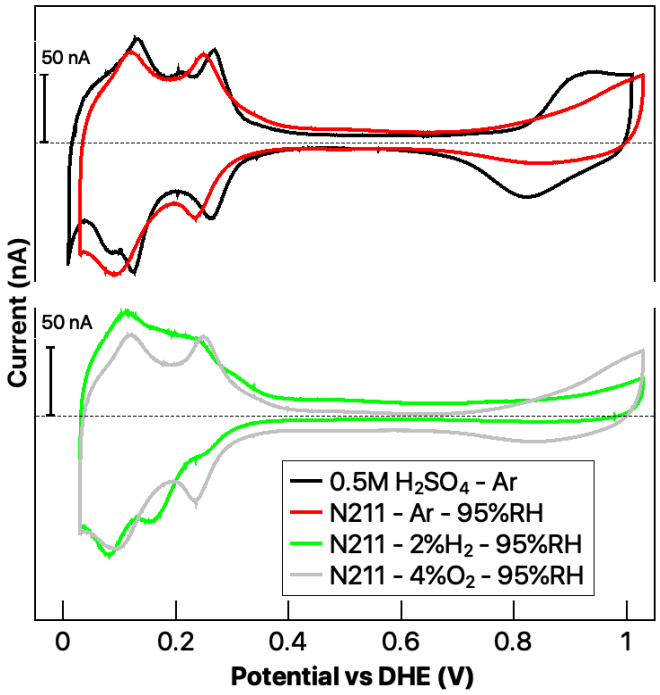

Figure 2. CV scans at 50 mV/s at various operating conditions. The applied mechanical pressure was 1.38 MPa (200 psi) when Nafion 211 was used. Solid-state cell was humidified at ~95% for measurements.

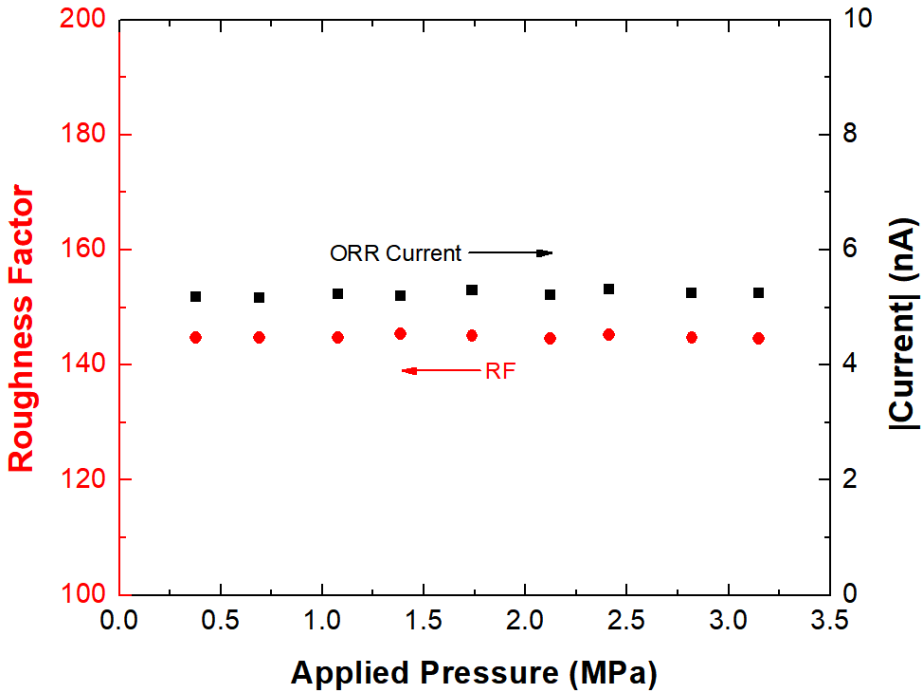

Figure 3. Effect of mechanical pressure on both roughness factor and ORR current. In both cases, no discernible trend is observed, with little absolute change in values across the 2.76 MPa (400 psi) range.

Effect of Mechanical Pressure on Roughness Factor and ORR

ECSA was measured as described in the Experimental section. The ECSA was then divided by the geometric area (GA) to obtain the roughness factor (RF). The roughness at different mechanical pressures is reported in Figure 3. RF remained relatively unchanged with increasing pressure, fluctuating around a value of 145. The slight variation in values is likely a result of measurement error. Below 0.34 MPa (50 psi), RF values were inconsistent and inaccurate and were omitted from this work. For comparison, the RF of the electrode in liquid was ~192. One potential reason for this difference is that the microelectrode is plated, which induces sub-micrometer features. In the aqueous cell, the liquid electrolyte can contact all of these features, increasing the area for adsorption/desorption and the measured current. However, in the solid-state cell, Nafion electrolyte is restricted to contact a more limited area of the electrode (the "peaks"), which results in a lower ECSA.

The change in the ORR current, measured using chronoamperometry, was also examined. Similarly, no significant trend was observed with applied pressure, with currents varying from ~5.17 to 5.31 nA across the 2.76 MPa (400 psi) range. These results demonstrate the mechanical robustness of our microelectrode cell. Even if the pressure varies slightly, electrode contact remains sufficient to produce consistent results. 1.38 MPa (200 psi) was chosen as the mechanical pressure to carry out all subsequent experiments.

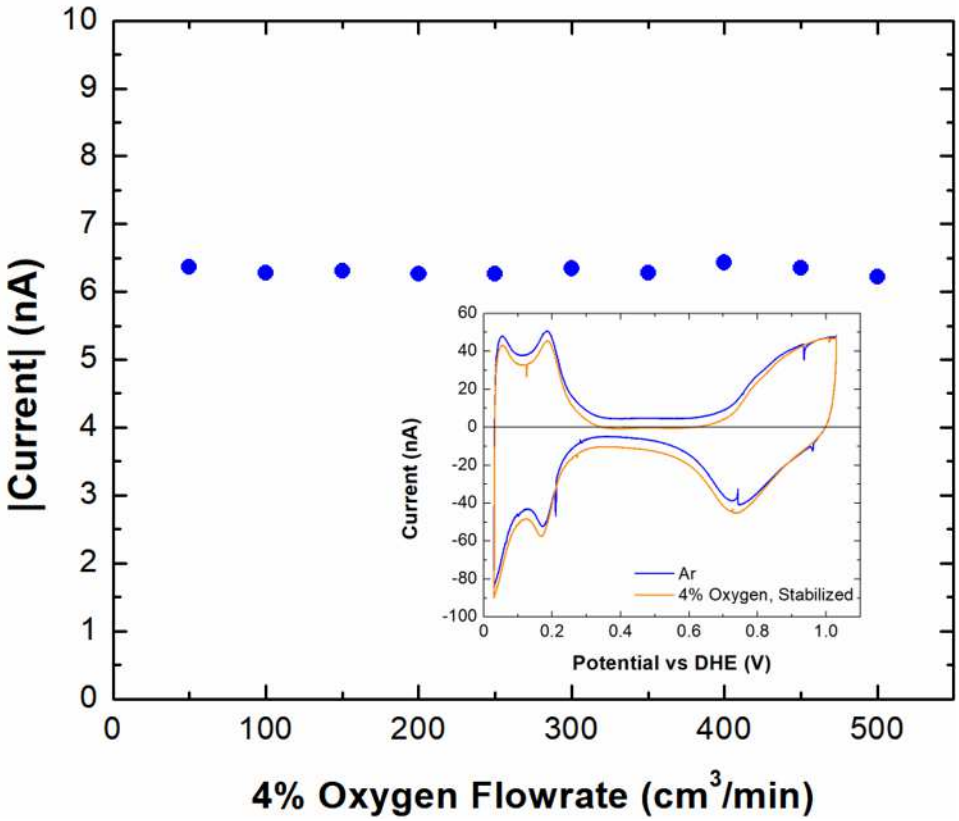

Figure 4. Plot of absolute value of ORR current versus oxygen gas flowrate. There is no discernible trend as flowrate increases. Inset plot shows CVs before and after switching from Ar to 4% O_2 gas. The O_2 gas CV stabilized after 7 cycles, approximately 12 min after the switch.

Effect of Gas Flowrate on ORR Current

To examine further the robustness of the experimental design, the 4% oxygen gas flowrate was varied, and the resulting ORR currents were measured via chronoamperometry (Figure 4). No significant trend was observed across a flowrate range as wide as 50 to 500 cm^3/min. Three things then become apparent. One, convection is not important in the system. Measured currents are diffusion-controlled, as expected. Two, the system is not oxygen limited, allowing for mass-transfer-limited currents to be determined. Three, changing the flowrate of the gas does not change the hydration of the membrane. Additionally, small fluctuations in flowrate as a result of mass-flow-controller error or other causes should have minimal impact on results.

Equilibration Time

One of the advantages of a flow-through UME cell compared with previous UME setups has been the equilibration time of the various cells. Equilibration times often are greater than 12 h (2, 5). One of the proposed benefits of our cell design is that the small volume and gas flow into the working electrode chamber dramatically reduces the time needed for the membrane to equilibrate. To test this hypothesis, a CV was taken at ~95% relative humidity followed by drying out the cell with 0% RH argon. The cell was then rehydrated, and additional CVs were performed. The results are shown in Figure 5 and demonstrate two major points. First, the system is highly responsive to changes in RH, as the CV taken at 0% RH has a very small magnitude and is highly resistive. Second, the membrane recovered quite quickly, with peaks reaching their previous level of magnitude after about 2 hours. It may have equilibrated faster if not limited by the humidifier itself. However, there was a significant shift in the reference electrode; after 2 hours, the reference shifted −110 mV, and after the overnight equilibration nearly −600 mV. This shift did not impact peak height or shape. It is unknown what caused this shift, but one possible solution is to humidify and control the gas flowing into the reference chamber, as this was not done in this experiment.

A second test was performed to ascertain equilibration of the system when switching from one gas to another (e.g., Ar to 4% O_2). To accomplish this, a CV scan at 20 mV/s was started under Ar at 95% humidity (see inset in Figure 4). During the scan, the gas was changed to 4% O_2, also at 95% humidity. The CV scan stabilized after just 7 cycles, which took about 12 min. Further work is needed to confirm the accuracy of these measurements and to determine what effect, if any, the CV experiment has on the time for equilibration.

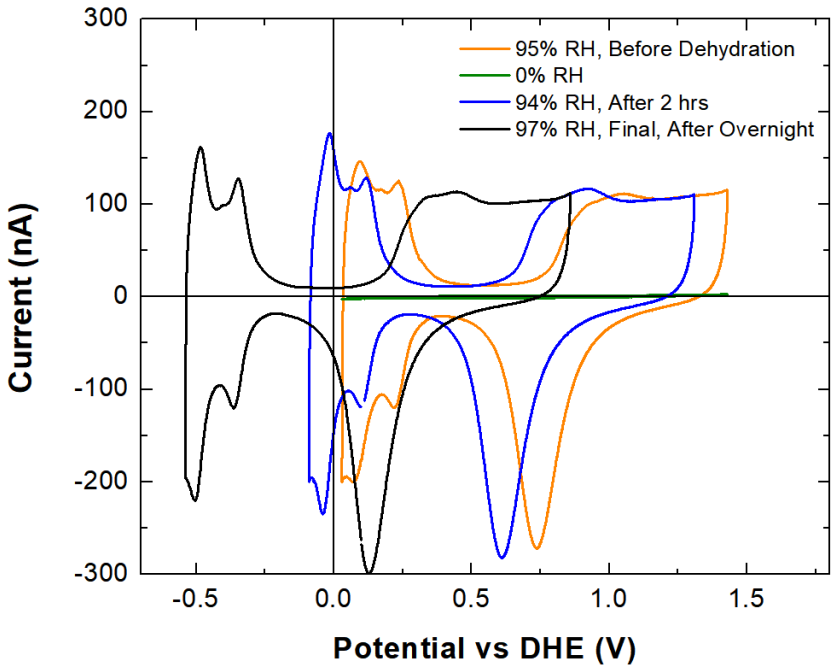

Figure 5. CVs taken both before and after dehydration of Nafion membrane. Scans are performed at 50 mV/s.

IR-Drop Measurements

Electrochemical impedance spectroscopy measured the IR drop in the microelectrode setup between the working and counter electrodes. From a plot of the imaginary part versus the real part of the resistance, the x-intercept was calculated by interpolation, resulting in an area-normalized resistance of 0.133 Ω-cm^2, which is expected for hydrated N211 (10). This resulted in an IR drop of -7.34×10^{-10} V, which is negligible in practice.

Summary

In this work, a new microelectrode cell for examining mass-transport resistances in ionomers and the kinetics of ORR and HOR was designed and tested. Both ORR and HOR behavior was observed, and this behavior did not change with mechanical pressure or gas flowrate. In addition, equilibration time was very small, potentially as low as 12 min when switching Ar to 4% O_2, although further work is needed to confirm this result. Finally, the measured IR drop in the cell was very small. These results demonstrate that the new microelectrode cell design is robust. Future work is focused on adapting methodology to other ionomers and discerning impacts of such variables as ionomer thickness and other electrochemical reactions.

Acknowledgements

This study was partially funded under the Fuel Cell Performance and Durability Consortium (FC-PAD) funded by the Energy Efficiency and Renewable Energy, Fuel Cell

Technologies Office, of the U.S. Department of Energy under contract number DE-AC02-05CH11231.

References

1. K. Kudo, R. Jinnouchi and Y. Morimoto, *Electrochim. Acta*, **209**, 682 (2016).
2. J. Chlistunoff and B. Pivovar, *J. Electrochem. Soc.*, **162**, F890 (2015).
3. A. J. Bard and L. R. Faulkner, *Electrochemical Methods: Fundamentals and Applications*, John Wiley & Sons, Inc., New York (2001).
4. A. Parthasarathy, C. R. Martin and S. Srinivasan, *J. Electrochem. Soc.*, **138**, 916 (1991).
5. D. Novitski and S. Holdcroft, *ACS Appl. Mater. Interfaces*, **7**, 27314 (2015).
6. J. Chlistunoff, *J. Power Sources*, **245**, 203 (2014).
7. A. Parthasarathy, S. Srinivasan, A. J. Appleby and C. R. Martin, *J. Electrochem. Soc.*, **139**, 2530 (1992).
8. P. D. Beattie, V. I. Basura and S. Holdcroft, *J. Electroanal. Chem.*, **468**, 180 (1999).
9. A. Kusoglu and A. Z. Weber, *Chem. Rev.*, **117**, 987 (2017).
10. J. Peron, A. Mani, X. Zhao, D. Edwards, M. Adachi, T. Soboleva, Z. Shi, Z. Xie, T. Navessin and S. Holdcroft, *J. Membr. Sci.*, **356**, 44 (2010).